SEISMIC DESIGN OF CUT-AND-COVER SECTIONS OF THE BAY AREA RAPID TRANSIT EXTENSION TO SAN FRANCISCO AIRPORT

FARHANG OSTADAN[1], JOSEPH PENZIEN[2]

ABSTRACT

Construction for the San Francisco Airport Extension of the Bay Area Rapid Transit (BART) District is underway at this time. The 13.5 km extension of the existing BART system will include 10 km of cut-and-cover subway box structure. The design for the cast-in-place reinforced concrete subway structure will include single-cell, double-cell, and wide boxes to accommodate multiple tracks. Also planned are two below-ground passenger stations and one at-grade station and one elevated station. The project alignment essentially parallels the San Andreas Fault at a distance of 2.5 km. A maximum credible earthquake with magnitude of 8+ is selected for design.

In this paper development of seismic design parameters in terms of racking displacement for the subway box is presented.

INTRODUCTION

Construction of the San Francisco Airport Extension of the Bay Area Rapid Transit (BART) District in underway and scheduled for completion in 2002. The extension is 13.5 km long passing through populated urban areas in the San Francisco Bay area. The extension and its vicinity are shown in Figure 1. The 13.5 km extension of the existing BART system will include 10 km of cut-and-cover subway box with stringent requirements for ground movement and vibration during excavation and shoring. The design for cast-in-place, reinforced concrete subway structure will include single-cell, double-cell, and wide boxes to accommodate multiple tracks. Also planned are two below-ground passenger stations (South San Francisco and San Bruno) and one at –grade station (Millbrae) and one elevated station (in San Francisco International Airport adjacent to the new constructed international terminal). The extension also includes aerial structures near the airport to go over Highway 101.

The subsurface profile typically consists of Quaternary alluvium overlying Colma formation, a thick sedimentary unit consisting primarily of dense, fine silty sand. The project alignment essentially parallels the San Andreas Fault at a distance of 2.5 km at the closest location. Following the approach used by BART, a Maximum Credible Earthquake (MCE) of magnitude 8+ is selected for design. BART design criteria require that the facilities be designed to withstand the effects of the MCE without significant degradation of the structural integrity. The system is expected to return to operation with minimal delay following a major earthquake in the area. The seismicity of the area and the performance requirement result in seismic loading levels well above those normally considered for such structures. For cut-and-cover subway box and the underground stations, the main component of the seismic loading is the racking displacement of the structure.

In this paper, development of seismic design parameter in terms of seismic racking displacement is discussed. A series of seismic soil-structure interaction (SSI) analyses were performed for various box

[1] Chief Soils Engineer, Bechtel, San Francisco, CA 94119, USA (fostadan@bechtel.com)
[2] International Civil Engineering Consultants, Inc., Berkeley, CA 94704, USA (penzien@icec.com)

structures and subsurface conditions. The results of analyses in terms of normalized racking ratios used for design are presented.

This paper is intended to present application of the SSI methodology for a major transportation project in a highly active seismic region of the world in order to develop a key seismic design parameter.

GEOLOGICAL AND SEISMOLOGICAL SETTING

The San Francisco Bay Area is located in central section of California Coast Range Physiographic Province near the west edge of the North American crustal plate. Past episodes of tectonism have resulted in folding and faulting of the characteristics of the Coast Range Province. During the past two million years there has been substantial change in the Bay Area landscape as a result of faulting, tectonic uplift, and subsidence. The post-Pleistocene rise in sea level during last 15,000 years formed San Francisco Bay and induced rapid deposition of sediments within the Bay and on the surrounding flat lands.

The geological units of interest in the project area from oldest to youngest include Franciscan Group, Merced Formation, the Colma Formation, Quaternary Alluvium and artificial fill. A major part of the BART alignment is in the alluvium. For this reason, the studies related to site conditions with alluvial deposits are presented.

Quaternary Alluvium typically consists of gray to brown sand and silt locally containing clay, gravel, or boulders. The estimated thickness of deposits ranges from few feet to over 100 feet, with the thickest deposits near the Bay.

The geotechnical investigation consisted of field sampling and testing including Standard Penetration Test (SPT), Cone Penetration Test (CPT) and geophysical measurement of soil dynamic properties. For the purpose of seismic design, the subsurface conditions along the alignment were divided into three classes. The site classes following the 1998 California Building Code (same as Uniform Building Code, 1994) are S1, S2 and a combined category of S3/S4 condition. Sites with alluvial deposits fall under S2 site class.

GROUND MOTION

The dominant feature with respect to seismicity, due to proximity and activity, is the San Andreas Fault located about 2.5 km along the alignment. A MCE with magnitude 8+ was assigned to the San Andreas Fault. Following an extensive study of the seismicity in the area and using the latest ground motion attenuation relationships, design ground motions were developed. The effect of the local soil conditions for various site classes were incorporated in the ground motion. The acceleration response spectra in the horizontal direction considered the directivity effect. In vertical direction, the design acceleration response spectrum was assigned to be 2/3 of the respective horizontal acceleration response spectrum, which was found to be adequate for the structural frequencies of interest. The acceleration response spectra for all three site classes are shown in Figure 2. A peak ground acceleration of 0.70g was adopted consistent with mean values obtained from the ground motion study.

Since time history analyses were needed, for each acceleration response spectrum, three sets of time histories (each with three components) were developed. The time histories, particularly in the fault normal direction, maintained a large velocity pulse to represent the near-fault effects due to directivity. The acceleration-compatible time history along with the velocity and displacement time histories of the S2 motion (for alluvial sites) corresponding to fault-normal direction (perpendicular to the alignment and in line with direction of shaking for racking) are shown in Figure 3. The directivity effect appears more pronounced in the velocity and displacement time histories.

SEISMIC RACKING ANALYSIS

It was recognized that ground deformation and the interaction between the structure and the surrounding soil control seismic loads in the underground structure. In order to facilitate the design process, it was decided to develop a set of normalized seismic racking curves recognizing the variation in soil properties and structural member sizes along the alignment and during the final design. The racking curves were obtained from a series of parametric SSI analyses using the Computer program SASSI (Ostadan et al., 2000). The results were compared with a quasi-static solution developed by Penzien (2000).

The strain-compatible soil shear modulus and damping values were obtained using the Computer program SHAKE (Schnabel et al., 1975). The initial and the strain-compatible shear wave velocity obtained from SHAKE analysis for the alluvial sites are shown in Figure 4. As shown in this figure due to high intensity of design motion, the strain-compatible shear wave velocity is significantly less than the initial velocity due to soil nonlinearity. In addition, SHAKE analysis results corresponding to various layers in the SHAKE model were processed and the profile of maximum relative displacement relative to ground surface was computed. The result is shown in Figure 5. The relative free-field maximum displacement is small at shallow depths and increases with depth. The maximum relative displacement profile was obtained for each point in the ground from the maximum value of the relative displacement time history (displacement time history of the point in the profile less the displacement at the ground surface). It was noted that the maximum value of relative displacement for all points would not occur at the same time. However, once a critical time for maximum displacement for a number of layers was identified, the maximum relative displacement values were found to be very close to the values at the critical time.

Following the free-field analysis, a series of SSI analyses were performed. A typical single-cell structure and the range of anticipated structural member dimensions are shown in Figure 6. The soil cover varies from 5 ft to 33 ft depending on the location.

The SASSI two-dimensional model of the single-cell structure is shown in Figure 7. The model has discrete soil elements on top of the box to assign appropriate soil properties for the replaced soil cover. There is no need to model the side soil and the soil below the structure with finite elements due to formulation of substructuring in SASSI and the internal models used to compute the impedance parameters.

The results of SSI analysis in terms of maximum angular distortion between the invert and the wall (γ_{max}) was computed. Computation of the maximum angular distortion ensures that the rigid body rotation of the structure is not included in the racking results. Once γ_{max} is obtained, the maximum racking displacement, $\Delta_{max,}$ may be obtained from

$$\Delta_{max} = \gamma_{max} * H \qquad [1]$$

where H is the height of the subway box structure.

The maximum racking ratio was obtained by dividing the maximum racking displacement of the structure by the maximum free-field relative displacement, $\Delta_{free\text{-}field}$, obtained from the results of Figure 5 corresponding to the elevation of the roof and invert of the structure in the ground as follows;

$$R = \Delta_{max} / \Delta_{free\text{-}field} \qquad [2]$$

In order to consider the structure and soil stiffness in normalized form, the flexibility ratio F was defined as

$$F = \frac{G_s \cdot W}{K_x \cdot H} \qquad [3]$$

where G_s is the strain-compatible shear modulus of the soil averaged over the height of the structure, K_x is the lateral stiffness of the box structure and W and H are the width and height of the box structure. Lateral stiffness K_x can be obtained from simple static analysis of the box structure without the surrounding soil under simple boundary condition as shown in Figure 8. Note K_x is the lateral stiffness per unit linear depth of the line axis. The flexibility ratio F defined above increases as the soil stiffness increases or the box stiffness reduces.

To verify the SSI results, the racking ratio obtained from SSI analysis was compared with the quasi-static solution by Penzien (2000) as shown in Figure 9. The results show a good agreement for the case considered. The quasi-static solution was developed based on the assumption of uniform soil properties and adequate soil cover on top of the box structure.

Following the verification of the results, the SSI analysis was extended to cover a wide range of structural and soil properties and soil cover depths. As a result of analysis, a set of racking curves shown in Figure 10 was established for seismic design of the single-cell structures. The design curves differentiate the effect of soil cover thickness at the thickness of 20 ft, which is approximately equal to the width of the box structure.

As depicted in Figure 10, for the flexibility ratio of one (box stiffness equals soil stiffness, see Equation 3), the racking ratio is also approximately one indicating racking of the box is the same as racking of the free-field soil. For stiffer structures (flexibility ratio less than one), racking of the structure is less than the free-field racking approaching zero for very stiff structures. On the other hand, for flexible structures (racking ratio larger than one), racking of the box is significantly larger than the ground free-field racking. For a deeply embedded cavity (a cavity with the shape of the structure with no stiffness) the racking ratio reaches a value between 2 and 3 (Penzien, 2000). This point should be noted since in the past it was assumed that the racking of the structure could not be larger than the free-field racking. The racking curves clearly show the SSI effects in various range of relative flexibility ratios.

Finally, while the racking increases by increasing the flexibility ratio, this increase may not necessarily cause an increase in the stresses in the structure. This is mainly due to reduction in the size of the structural members (thus causing increase of flexibility ratio) resulting in smaller stresses for a larger racking value. To illustrate this point, the bending stresses in the walls due to seismic racking are plotted for various widths of the wall thickness along with the racking curve in Figure 11. As shown in this figure, the seismic bending stresses are small for small flexibility ratio primarily caused by larger member sizes (wall thickness of 3 ft and above). The bending stresses are also small for large racking ratios even though the amount of racking is larger. This is caused primarily by the small size of the wall thickness having smaller sectional modulus. The seismic bending stress is largest for a wall thickness of about 1.8 ft as shown in Figure 11. This thickness corresponds to the flexibility ratio of 3.5 and is in the mid-range of predicted racking ratios. For design purposes results such as those shown in Figure 11 can be combined with the stresses caused by other applicable loads (static soil pressure, overburden pressure, operational loads, etc.) to optimize the sections in terms of structural member sizes and the steel.

In order to incorporate the seismic load in the design, the designer needs to follow the following simple steps

1. Use a structural analysis program to obtain the lateral stiffness, K_x, of the structure with simple boundary conditions shown in Figures 8.
2. From the strain-compatible soil properties, shown in Figure 4, obtain the average shear modulus of the soil layer, G_s, in the depth range of the structure in the ground.
3. Determine the flexibility ratio F of the proposed structural design using Equation (3).
4. Determine the racking ratio from Figure 10.

5. Determine the difference of maximum free-field relative displacements corresponding to the top and the bottom elevations of the proposed structure from Figure 5, then multiply this differential displacement by the racking ratio obtained from Step 4. The value obtained is the design racking displacement of the structure under consideration.
6. Apply the racking displacement as input in the structural model of Step 1 to obtain the shear, moment and other structural design parameters.
7. Optimize the design by evaluating the stresses for an applicable range of structural member sizes.

The same procedure was followed for double-cell and triple-cell structures with simple steps for designer to follow and obtain seismic loads. Similarly for the underground stations, both single and multi-level stations, corresponding racking ratios were obtained and used in design. For stations at end sections it was recognized that presence of cross walls stiffens the sections considerably. For such sections, the seismic soil pressure distribution obtained from the SSI analysis was used in design. The outcome of the study is summarized in the BART seismic design criteria, which was used as part of contract document for the design-build contract under construction at this time.

SUMMARY

Selected parts of an extensive study to develop key seismic design parameters for a major transportation project in a highly active seismic region of the world are presented. The main reason for the selection was to illustrate the application of the soil-structure interaction approach used in developing a robust and practical parameter for assessing the seismic response of under ground structures. The approach is significantly different and results in a completely different design when compared with the conventional force method based on seismic soil pressure used for such structures in the past. The results also show that the assumption of using free-field deformation for design may be unduly conservative or may severely underestimate racking displacement depending on the relative flexibility (or stiffness) of the soil and the structure.

REFERENCES

Penzien, J. (2000), “Seismically induced racking of tunnel lining,” Earthquake *Engineering and Structural Dynamics*, Vol. 29, pp. 683-691.

Ostadan, F.; Chin, C.; Lysmer, J. (2000), “SASSI2000-A System for Analysis of Soil-Structure Interaction,” University of California, Berkeley, CA, USA an Improved Version of original SASSI, Lyermer et al. (1981), Report UCB/GT/81-02, Geotechnical Engineering, University of California, Berkeley, April.

Schnabel, P. B.; Lysmer, J.; Seed, H. B. (1972), “SHAKE-A Computer Program for Earthquake Response Analysis of Horizontally Layered Sites,” Report No. EERC 72-12, Earthquake Engineering Research Center, UCB, December.

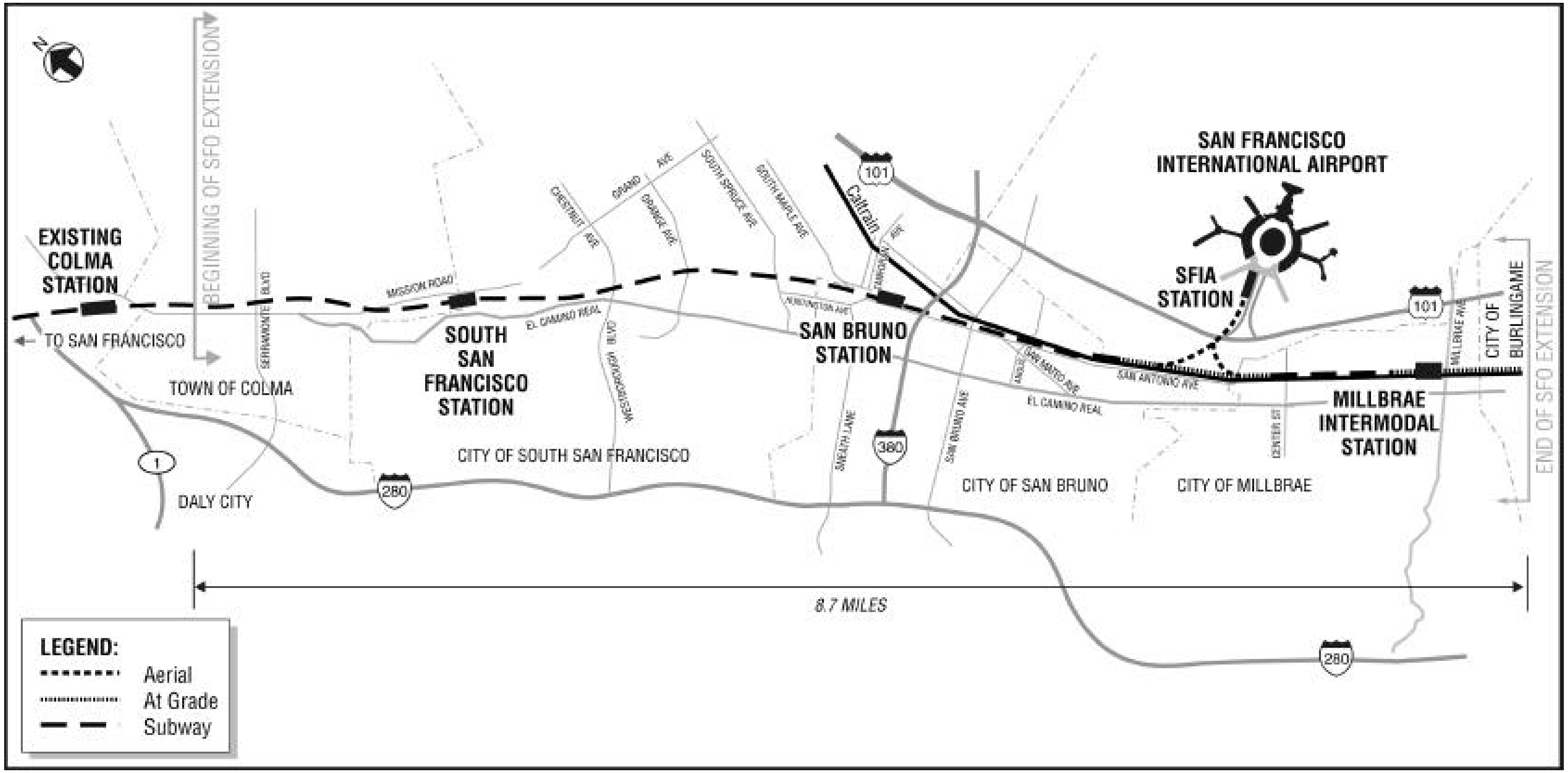

Figure 1. Project Location

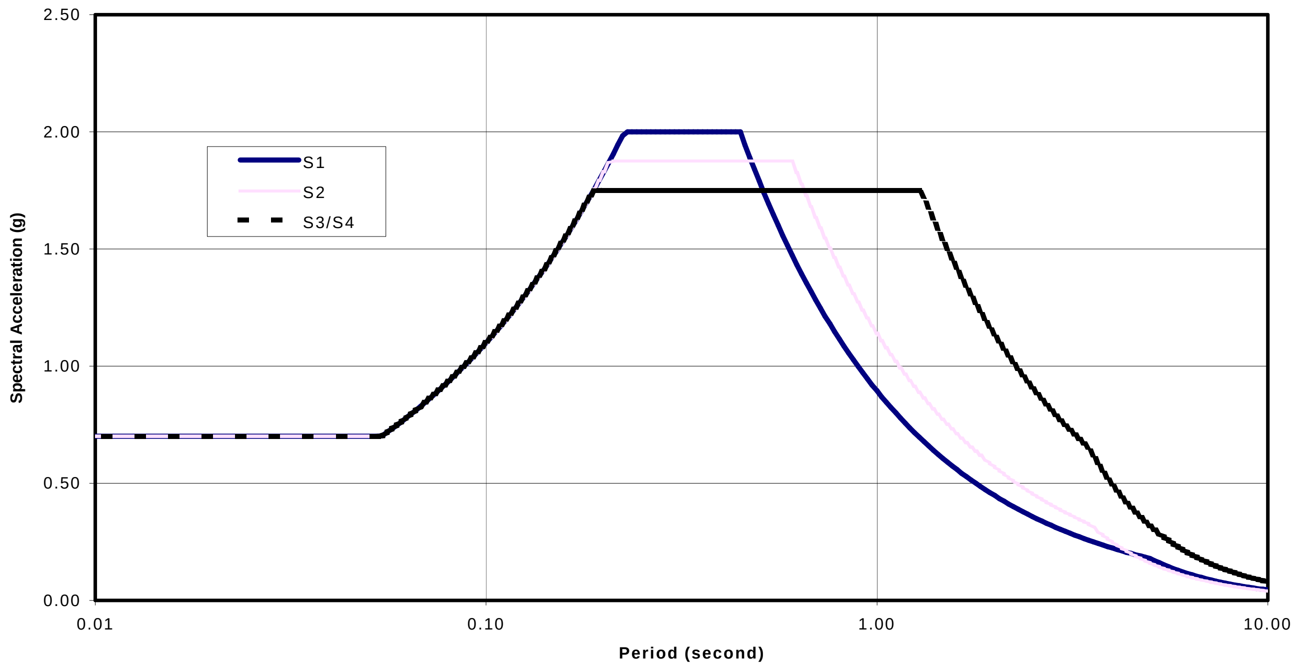

Figure 2. SFO BART Extension Design Response Spectra

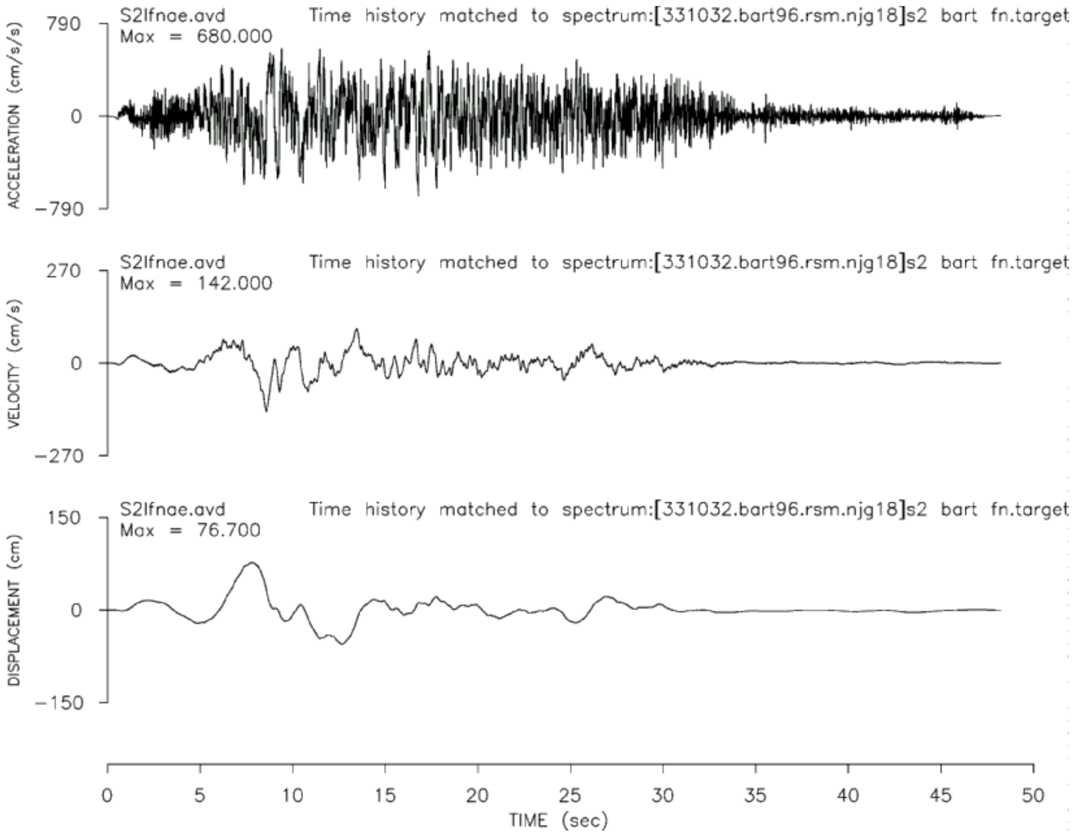

Figure 3. Acceleration, Velocity and Displacement Time Histories for S2 Fault-Normal Component

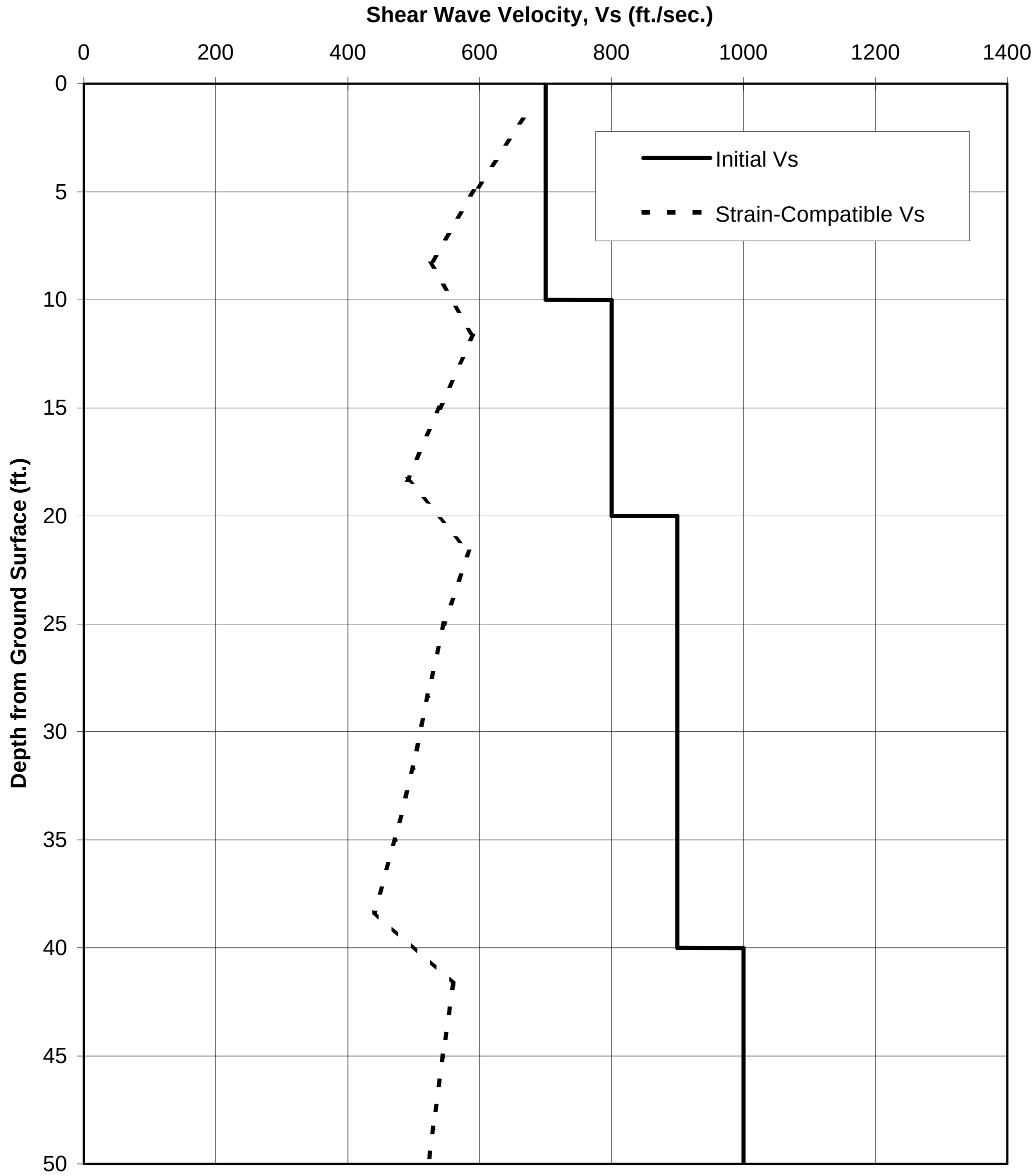

Figure 4. Initial and Strain-Compatible Shear Wave Velocity for Alluvial Sites

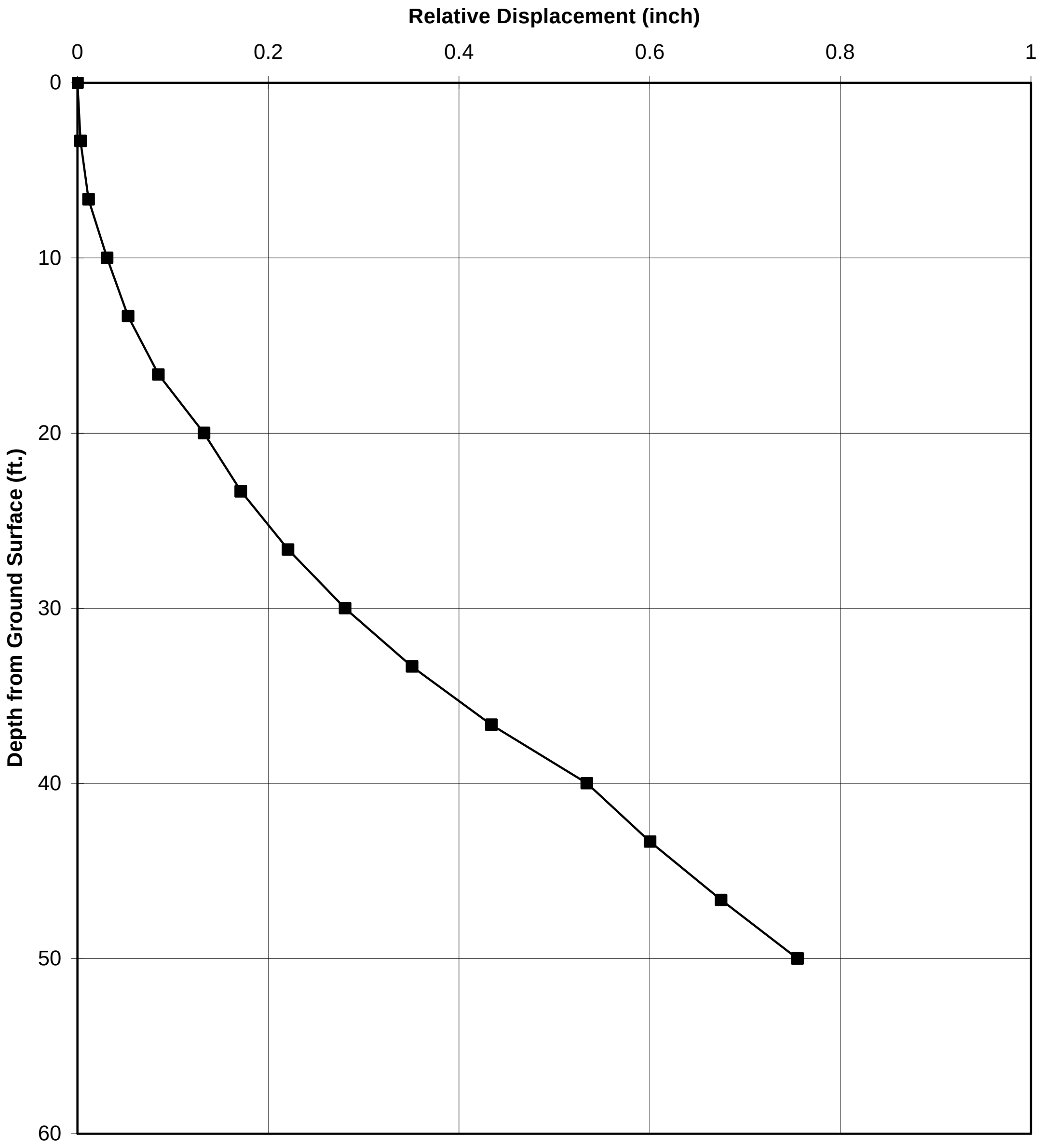

Figure 5. Maximum Relative Displacement in Free-Field for Alluvial Sites

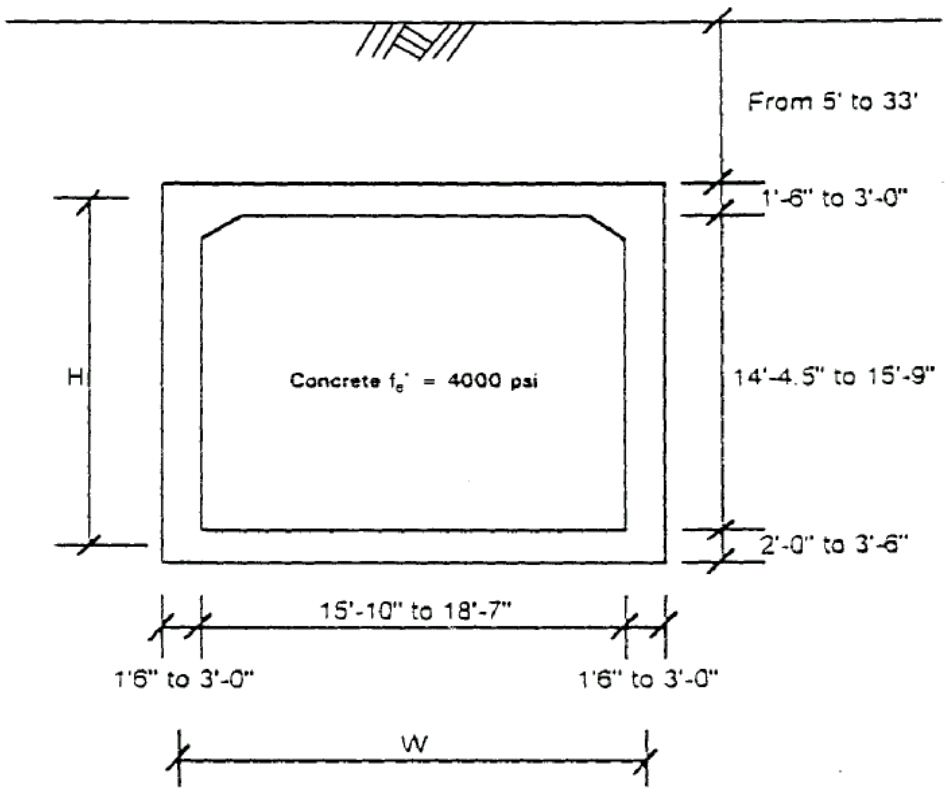

Figure 6. Typical Single-Cell Configuration

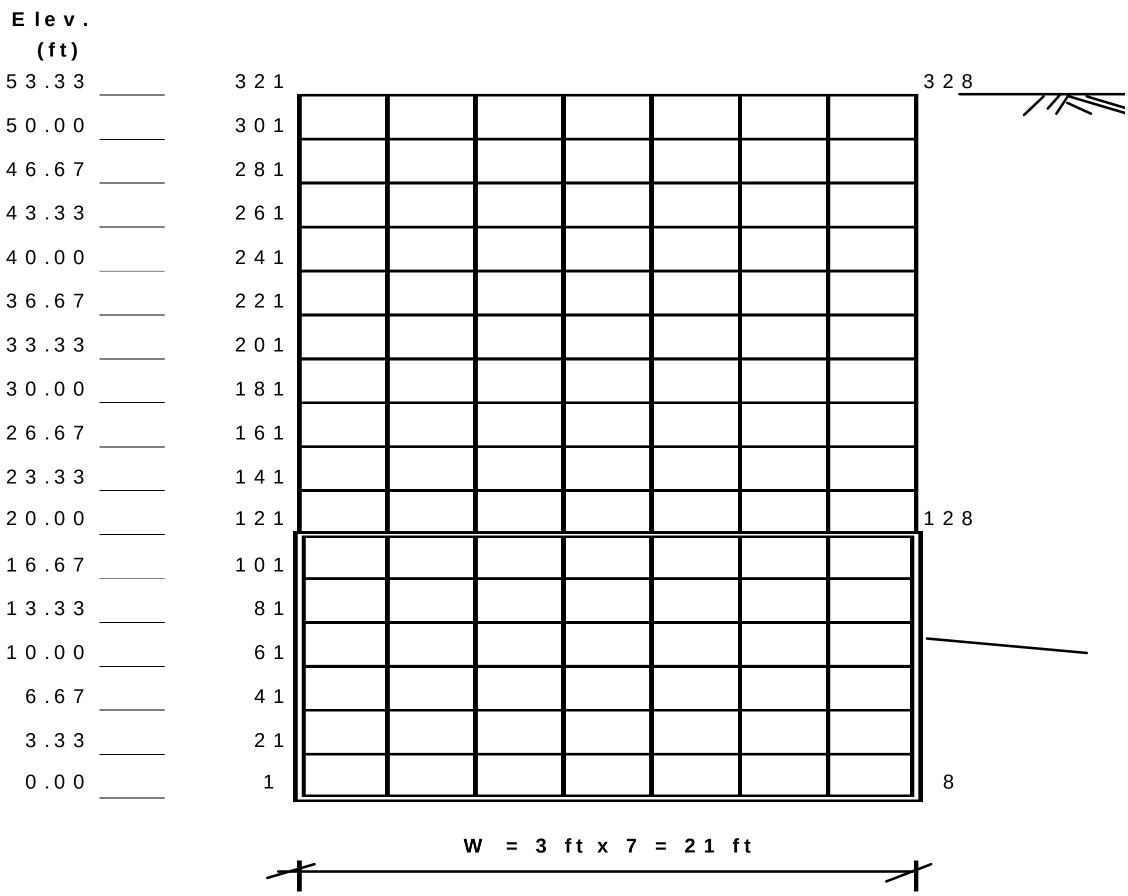

Figure 7. SASSI Model of the Single-cell Structure with 33 Ft Soil Cover

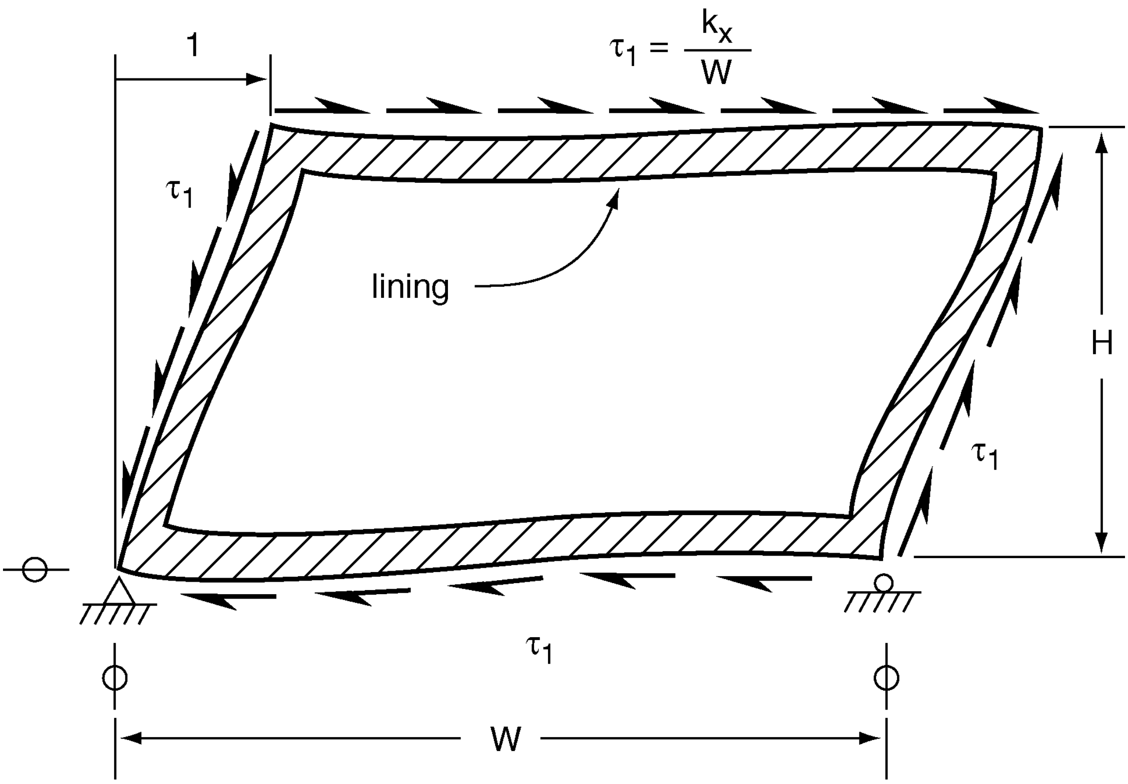

Figure 8. Simple Boundary Conditions to Obtain Lateral Stiffness of the Structure and Also Develop Seismic Shear and Moment for Members

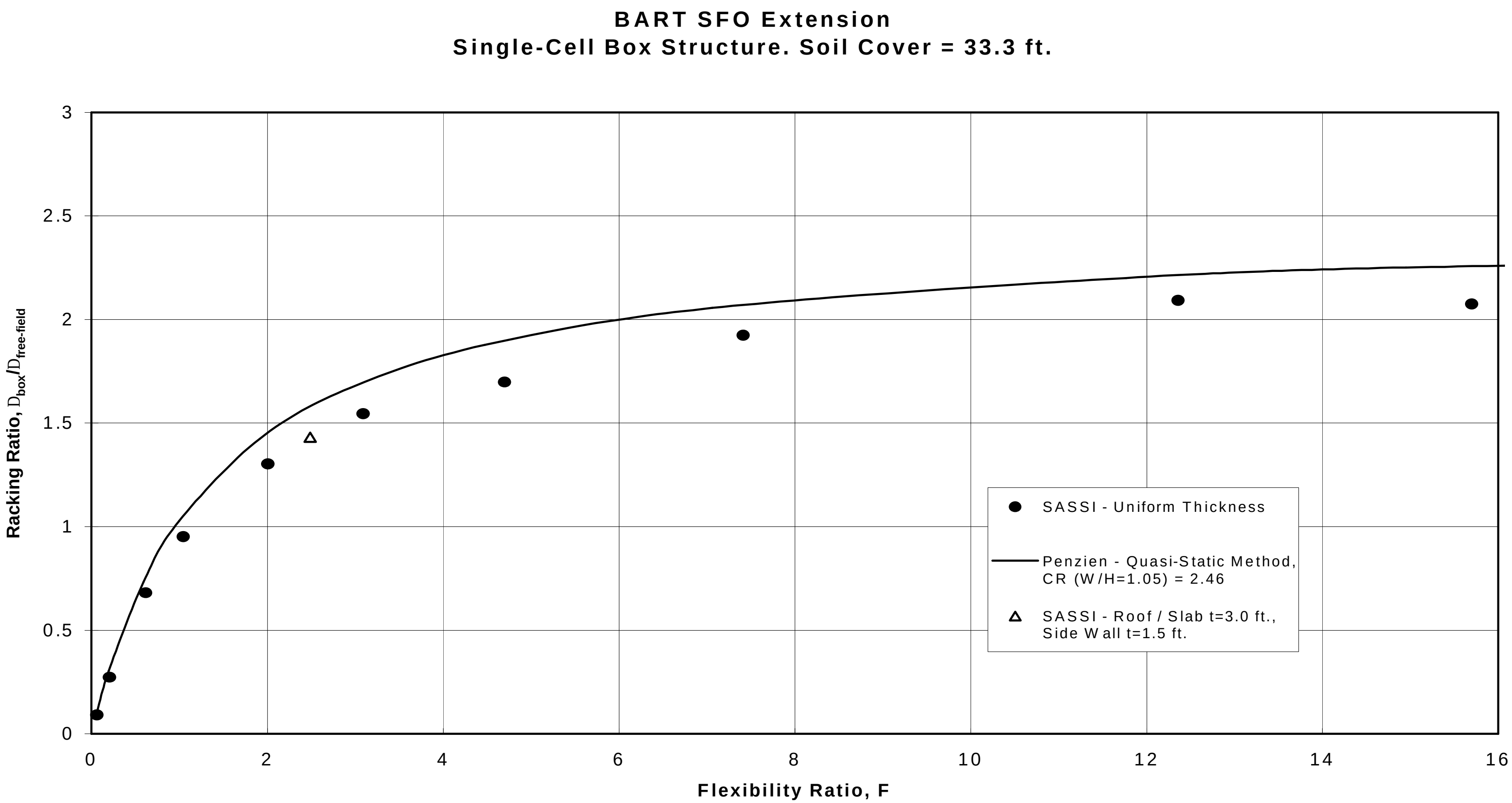

Figure 9. Comparison of Racking Ratios from SASSI and Penzien (2000) for Single-Cell Structure with 33 ft Soil Cover

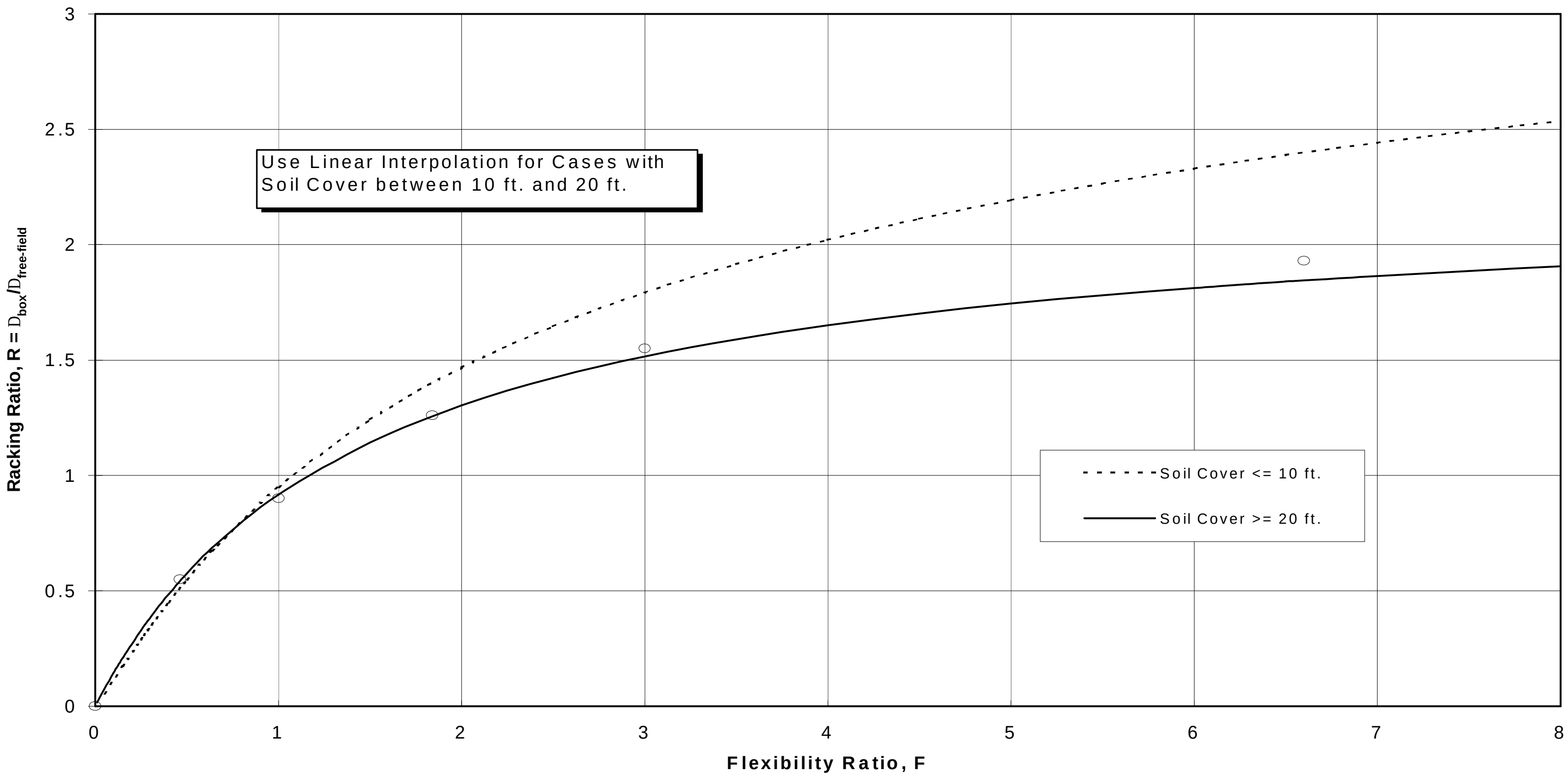

Figure 10. Recommended Racking Curves for Single-Cell Structures in Alluvial Soils

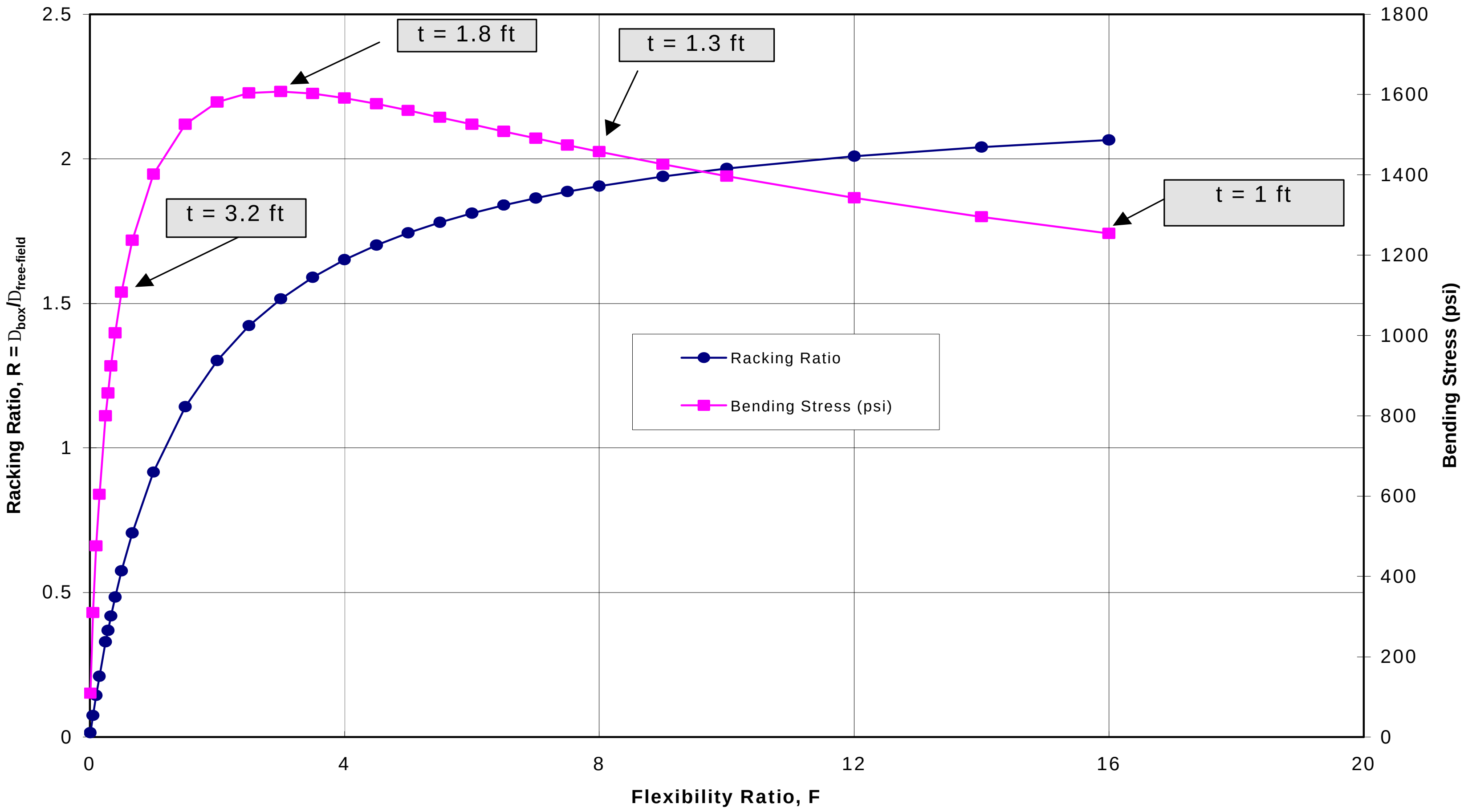

Figure 11. Seismic Racking and Bending Stresses in the Walls